First-Principles Studies on Carbon Nanotubes Functionalized with Azomethine Ylides

ARTICLE *in* THE JOURNAL OF PHYSICAL CHEMISTRY C · JULY 2008

Impact Factor: 4.77 · DOI: 10.1021/jp710938v

3 AUTHORS, INCLUDING:

Seokmin Shin
Seoul National University
109 PUBLICATIONS **1,678** CITATIONS

SEE PROFILE

First-Principles Studies on Carbon Nanotubes Functionalized with Azomethine Ylides

Eunseog Cho, Seokmin Shin, and Young-Gui Yoon*

School of Chemistry, Seoul National University, Seoul 151-747, Korea, Department of Physics, Chung-Ang University, Seoul, 156-756, Korea

Received: November 16, 2007; Revised Manuscript Received: March 15, 2008

Theoretical studies based on density functional theory framework have been performed on covalently functionalized carbon nanotubes (NTs) with azomethine ylides using SIESTA and CPMD codes. In view of the binding energies, it is found that armchair tubes favor functionalization at C−C bonds slanted to the tube axes, whereas zigzag NTs prefer attachment of the ylides at segments parallel to the tube axes. It is also suggested that the geometry of pyrrolidine rings attached to NTs strongly depends on the binding segments. The dependency is attributed to the degree of π-orbital alignment. Comparison of various functionalized derivatives on armchair tubes shows that the binding segments and atomic types at the segments significantly influence the electronic band structures near the Fermi energy. In metallic NTs, the covalent functionalization leads to opening of band gaps, whereas the effect of functionalization on the change of band gap energies is negligible for semiconducting NTs.

Introduction

During the past few years, intense attention has led to the achievement of covalent and noncovalent chemistry on the sidewall of carbon nanotubes (NTs).[1] A wide range of covalent functional groups such as hydrogen,[2] fluorine,[3] OH,[4] COOH,[5] ozone,[6] nitrenes,[7] carbenes,[8,9] and radicals[10] have been attached on the sidewall of nanotubes. Experimental and theoretical investigations reveal that the covalent modification permits the presence of local sp^3 hybridization or bond breaking on the tube sidewall that may lead to chemically modified new nanobased materials, while the noncovalent functionalization preserves the structural properties of nanotubes.[11] In addition to the studies of the sidewall chemistry, some researchers have investigated the functionalization of defect sites of nanotubes with open tips and have suggested that open-ended NTs have greater adsorption capacity than the closed-ended NTs, since the defect edges are generally more reactive.[12,13]

Recently, Prato et al. designed a new approach based on 1,3-dipolar cycloaddition of azomethine ylides ($H_2C{=}N^+RC^-H_2$) derived from condensation of an α-amino acid and an aldehyde.[14] They showed that the resulting products have remarkably high solubility in most organic solvents and even in water. The reaction has been widely applied to various azomethine ylides including N-protected amino acids such as ferrocene-modified glycine precursor,[15] which leads to diverse applications in the fields of solar energy conversion and selective anion recognition.[16] Biological moieties can be attached to the functionalized tubes using this chemistry and have been explored for medical fields such as diagnostics, vaccine delivery, and gene transfer.[17] In addition to Prato's method, an alternative scheme for synthesis of the functionalized NT with azomethine ylides generated by trialkylamine-N-oxides was recently reported by Mioskowski et al.[18] They proposed a new scheme for the separation of semiconducting NTs from metallic tubes with azomethine ylides in the presence of lignoceric acid. While extensive efforts are directed toward functionalized NTs involving azomethine ylides using different experimental techniques, few studies using theoretical investigations have been reported in the literature.

Theoretically, Lu and his co-workers attempted to determine transition states and binding energies of 1,3-dipolar cycloaddition of a series of 1,3-dipoles including azomethine ylide on metallic NT by means of two-layered ONIOM (our own n-layered integrated molecular orbital + molecular mechanics) approach.[19] Some questions, however, still remain unsolved about the structural and electronic properties on the functionalized NTs containing azomethine ylides. In particular, little is known about characteristics of band structures, preferential binding configurations, local geometries, and the effects of long-chain functional groups on the functionalized NTs. We performed first-principles electronic structure calculations and molecular dynamics simulations to address those issues.

Method

We have mainly used the SIESTA[20] code, capable of fully self-consistent density functional calculation to solve the standard Kohn−Sham equations using a basis set of numerical atomic orbitals. Standard norm-conserving pseudopotentials generated according to the procedure of Troullier and Martins is used to describe the ion−electron interaction. We have considered an energy cutoff of 120 Ry and a split-valence double-ζ basis set plus the polarization functions. We have also used the CPMD[21] method with Vanderbilt ultrasoft pseudopotentials and energy cutoff of 25 eV to perform dynamics simulations. In both methods, we adopted the generalized gradient approximation (GGA) implemented by Perdew, Burke, and Ernzerhof (PBE)[22] for the exchange-correlation energy functional. To simulate one-dimensional infinite functionalized NTs, periodic boundary condition is applied along the tube axis (z-direction) and vacuum spaces well above 5 Å are used in the x,y-directions. The Monkhorst and Pack scheme of k-point sampling is used for integration over the first Brillouin zone, and four k-points along the tube axis are used for all tubes in self-consistent calculations. All tubes are fully relaxed until all

* Author to whom correspondence should be addressed. E-mail: yyoon@cau.ac.kr.

10.1021/jp710938v CCC: $40.75
Published on Web 07/11/2008

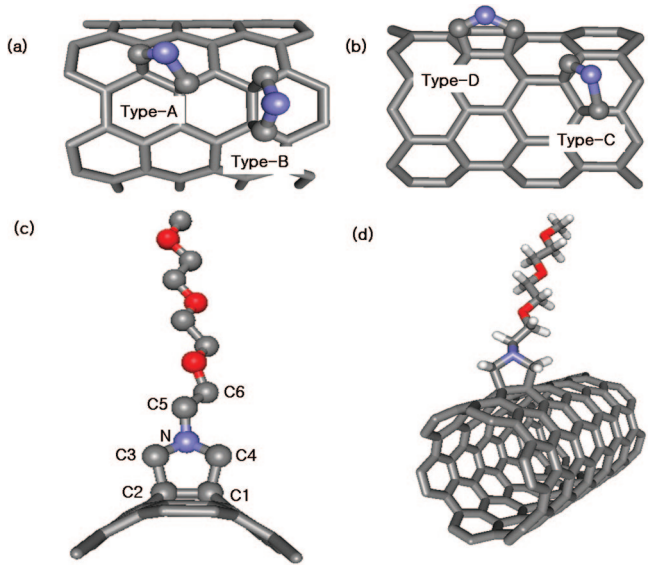

Figure 1. (a) Azomethine ylides attached to an armchair (n, n) nanotube. (b) Azomethine ylides attached to a zigzag (n, 0) nanotube. (c) Local structure of (6, 6) type-A MeO_NT. (d) Optimized geometry of (6, 6) type-A MeO_NT. Carbon, oxygen, nitrogen, and hydrogen atoms are in gray, red, blue, and white color, respectively. Hydrogen atoms are omitted for clarity in (a)−(c).

force components are smaller than 0.025 eV/Å and about 30 k-points are used to plot the band structures.

Results and Discussion

A. Structures and Binding Energies. We selected (4, 4) and (6, 6) armchair tubes as well as (8, 0) and (9, 0) zigzag tubes. The number of unit cells of armchair tubes used to generate supercell is six, and three units for zigzag tubes are chosen to be consistent with experimental results. Experimental data show the number of pyrrolidine rings on the NT surface is one group per 100 carbon atoms of the NT.[14] It is noted that supercells of both (4, 4) and (8, 0) single-walled NTs we calculated contain 96 carbon atoms, and those of (6, 6) and (9, 0) tubes include 144 and 108 carbon atoms, respectively. All tubes are fully relaxed. First, we have calculated the functionalized nanotubes with dichlorocarbene (CCl_2_NT) to check the validity of the parameters we adopted, and have found good agreement with the previous results in the literatures.[8,9] In our approach, we focus on functionalized NTs with an azomethine ylide including three oxygen atoms similar to ether derivative (R: $CH_2CH_2OCH_2CH_2OCH_2CH_2OCH_3$; MeO_NT) synthesized by Proto et al. For comparison, we have also studied two substituted forms. One form is simple azomethine ylide functionalized NT (R: H; H_NT) and the other is complicated form (R: $CH_2CH_2OCH_2CH_2OCH_2CH_2NHCOFc$; Fc_NT) containing the ferrocene-modified functional group. This hybrid material shows photoinduced intramolecular electron transfer from ferrocene group to nanotube leading to long-lived ($Fc^{\cdot+}$)-($NT^{\cdot-}$) species.[15] The charge separation property can be used in solar energy harvesting and specific anion recognizing applications. The binding energy E_b between an addend and the carbon nanotube is defined as $E_b = E[\mathrm{NT}] + E[\mathrm{addend}] - E_{\mathrm{total}}[\mathrm{NT} + \mathrm{addend}]$, where E_{total} is the total energy of the system per supercell. Figure 1 shows the different binding configurations for armchair (Figure 1a) and zigzag (Figure 1b) nanotubes, a local structure (Figure 1c), and an optimized structure (Figure 1d) of a functionalized nanotube. Hydrogen atoms are omitted for clarity in Figure 1a−c. We define a binding segment as a line segment joining a pair of carbon atoms of a nanotube to which an addend is attached. For armchair tubes, a configuration with a binding segment slanted from the tube axis is defined as type-A while a configuration with a binding segment perpendicular to the tube axis is defined as type-B. For zigzag tubes, a configuration with a binding segment slanted from the tube axis is defined as type-C while a configuration with a binding segment parallel to the tube axis is defined as type-D. The binding geometries and energies with functionalized NTs containing the azomethine ylide (MeO_NTs) are summarized in Table 1. Generally, azomethine ylides undergo 1,3-diploar cycloaddition to olefins to give pyrrolidine derivatives in good yields. The pyrrolidine molecules have two forms: one is a twisted (type-T) which has dihedral angle θ (C4−C1−C2−C3) of 89.9°; the other is an envelope (type-E) form whose dihedral angle is 0°.[23] It is known that the energy difference of two types is very small; hence, they can be interconverted in the ambient conditions. It is noteworthy that all pyrrolidine rings generated on slanted binding segments (type-A, type-C) have twisted forms, but the rings with binding segments perpendicular (type-B) or parallel (type-D) to the tube axis have only envelope forms. The π-orbitals of adjacent nanotube atoms whose segment is perpendicular or parallel to the tube axis are aligned. Therefore, in type-B and type-D configurations, two carbon atoms of addends, covalently bonded on the segments, also have the same type of alignment of π-orbitals. The alignment leads to envelope forms. The dihedral angles of type-B and type-D configurations are very similar to the angle of the envelope form (type-E) of pyrrolidine molecule. However, the rings attached to the C−C bond slanted to the tube axis (type-A, type-C) have much smaller dihedral angles (~25°) than that of optimized twisted (type-T) pyrrolidine molecule. It is well-known that NTs have π-orbital misalignments at the bonds that are neither parallel nor perpendicular to the tube axis, which allows addition reactions on the sidewalls of NTs through the relief of the strain of walls. It is reported that the π-orbital misalignment angles in (6, 6) tubes are 17.6° and the values for the (5, 5) and (10, 0) tubes are 21.3° and 18.5°, respectively.[24] These are very similar to the dihedral angles (~25°) of the addends attached to the C−C bond slanted to the tube axis. We conclude that the local geometry of pyrrolidine rings attached to the NTs is determined by the degree of π-orbital alignments on the binding segment of the pristine nanotube rather than the stable geometries of pyrrolidine molecules. In all azomethine ylides systems, the C1−C2 bond lengths are around 1.57 to 1.71 Å (Table 1), which is significantly larger than the C−C bond lengths of 1.42 Å with sp^2 character on the pristine tubes and also a little larger than those of type-T (1.53 Å) and of type-E (1.54 Å) of pyrrolidine molecules with sp^3 character. As the addends make the covalent bonds with the carbon atoms on the sidewall, the C1−C2 bonds are elongated and atomic character at the sites changes from sp^2 to sp^3 hybridization. Comparison of binding energies for metallic tubes indicates that the configuration with slanted π-orbital misalignment (type-A) is more stable than the configuration with π-orbital alignment (type-B), whereas the trend is reversed in the semiconducting tubes; for (n, 0) tubes, the type-D configuration is more stable than the type-C configuration. In CCl_2 metallic systems (CCl_2_NTs), the type-B configuration is more stable than the type-A, and difference of binding energies (~0.73 eV) is larger than that of azomethine ylides systems. For CCl_2 tubes, the type-A configuration generates triangular rings which produce higher-energy structures due to large ring strain, whereas the functionalization of CCl_2 on the type-B configuration causes

TABLE 1: Characteristic Bond Lengths (C1−C2), Angles (C3−N−C4), Dihedral Angles θ(C4−C1−C2−C3), and Binding Energies (E_b) of Functionalized Nanotubes (MeO_NTs) with Azomethine Ylide Derivatives

NTs	diameter (Å)	type	C1−C2 (Å)	C3−N−C4	θ(C4−C1−C2-C3)	E_b (eV)
(4, 4)	5.42	A	1.58	106.4	28.6	1.54
		B	1.71	103.9	1.9	1.29
(6, 6)	8.14	A	1.57	107.3	27.9	0.71
		B	1.65	103.7	1.2	0.46
(8, 0)	6.26	C	1.63	109.3	24.2	0.79
		D	1.57	105.3	0.5	1.40
(9, 0)	7.05	C	1.65	109.3	26.0	0.78
		D	1.57	108.1	0.4	1.11
pyrrolidine[23]		T	1.53	109.6	89.9	−
		E	1.54	105.6	0.0	−

the sidewall bond to be broken and makes relatively stable seven-membered rings with sp^2 carbons at the binding segment. The attachment of azomethine ylides, however, produces five-membered pyrrolidine rings with small ring strain in all types, which makes two types closer in energy than those of metallic CCl_2_NTs. It is found that the binding energy of the azomethine ylide onto (4, 4) and (6, 6) tubes varies significantly. However, the binding energy onto (8, 0) and (9, 0) tubes is very similar. For metallic tubes, both types have the same difference in binding energy of 0.83 eV; for semiconducting tubes, the differences of type-C and type-D are 0.01 and 0.29 eV, respectively. It is well-known that the larger the diameter of the nanotube is, the lower the binding energy of the functionalized NT is. In Table 1, the diameter of a (6, 6) tube is 2.72 Å larger than that of a (4, 4) tube, and the diameter of a (9, 0) tube is 0.79 Å larger than that of a (8, 0) tube. It is reasonable that differences between binding energies of (4, 4) and (6, 6) tubes are larger than those between binding energies of (8, 0) and (9, 0) tubes, which supports the statement that the binding energies depend on the diameters of NTs.

B. Electronic Structures and CPMD Results. Figure 2 shows the band structures of metallic (4, 4) tubes functionalized with a azomethine ylides (MeO_NTs) per six-unit supercell. The single addition on the binding segment slanted from the tube axis (type-A) leads to band gap opening at Γ point at the Fermi level, making it semiconducting, whereas the type-B configuration is metallic. The feature is understandable because the type-A configuration breaks a mirror symmetry of the nanotube, while the type-B configuration maintains the symmetry locally after functionalization. Figure 3 shows the band structures of metallic (6, 6) tubes functionalized similarly. The single addition on the slanted binding segment gives rise to degeneracy at Γ point (type-A), and the degeneracy is lifted as the further attachment is allowed on the opposite side of the first functionalization (type-AA). For type-AA, a pyrrolidine ring is attached per 72 carbon atoms of NT. Mioskowski et al. reported an appreciably increased fraction of carbon atoms bearing a covalently bonded moiety.[18] The fraction of type-AA we calculated seems to be reasonable in view of their experiment. On the other hand, the type-B configuration has the a band structure similar to that of pristine tube near the Fermi level, which is consistent with the band structure of type-B for the (4, 4) tubes.

The various type-A band structures of (6, 6) tubes with four-unit supercell have been calculated with different substitutes shown in Figure 4. In this case, the number of atoms of NT per addend is the same as that of Prato's experiment. All structures generate considerable band gaps which are different from the results of the six-unit supercell calculation. In the MeO_NT, the flat bands originating from organic chains are produced below ∼2 eV from Fermi energy. Fc_NT has a pair of distinct flat bands just below the Fermi energy originating from the Fe atom of the ferrocene ring. The bands can play an important role in excited-state charge transfer from addends to NTs.[15] It

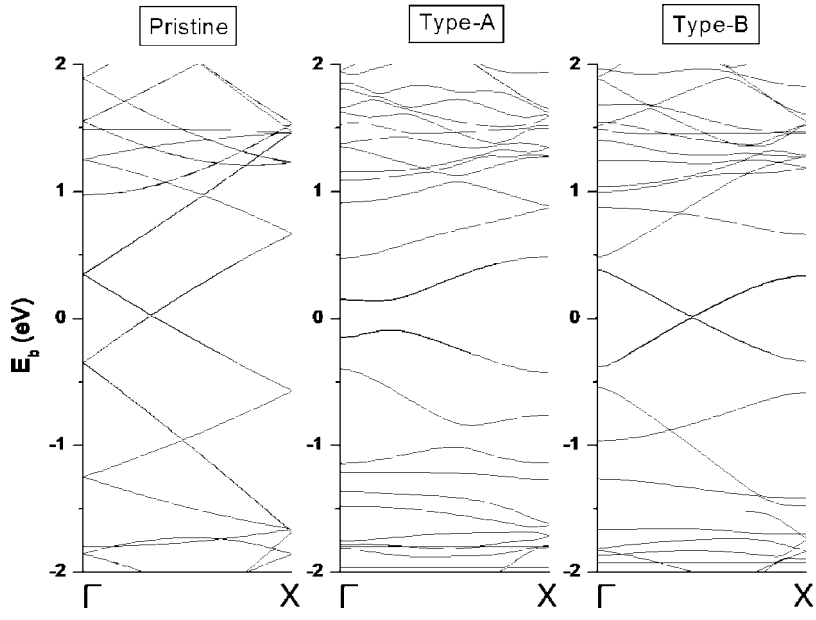

Figure 2. Band structures of pristine (4, 4) nanotube (left), type-A (middle), and type-B (right) armchair (4, 4) MeO_NTs.

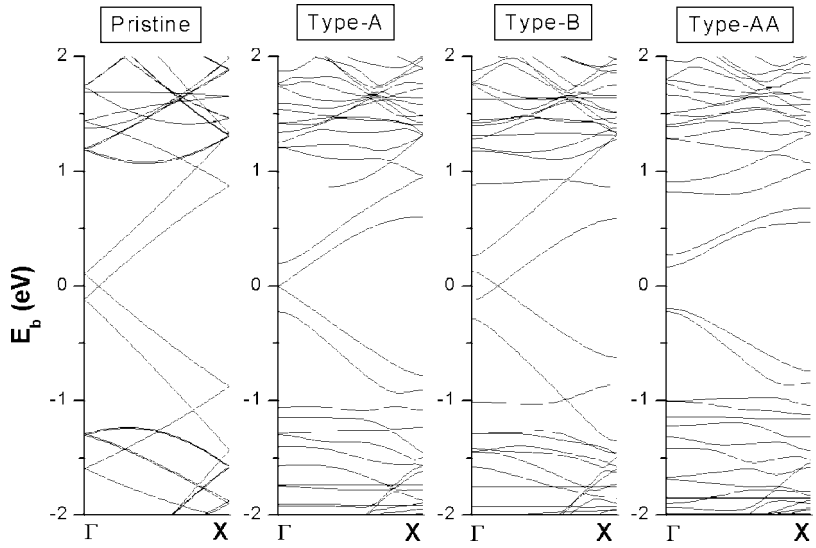

Figure 3. From left to right, the band structures on pristine, type-A, type-B, and type-AA functionalized NTs (MeO_NTs) are shown. For type-AA, the second addend is attached to the opposite position of the first functionalization. The band structures are calculated for six-unit supercells.

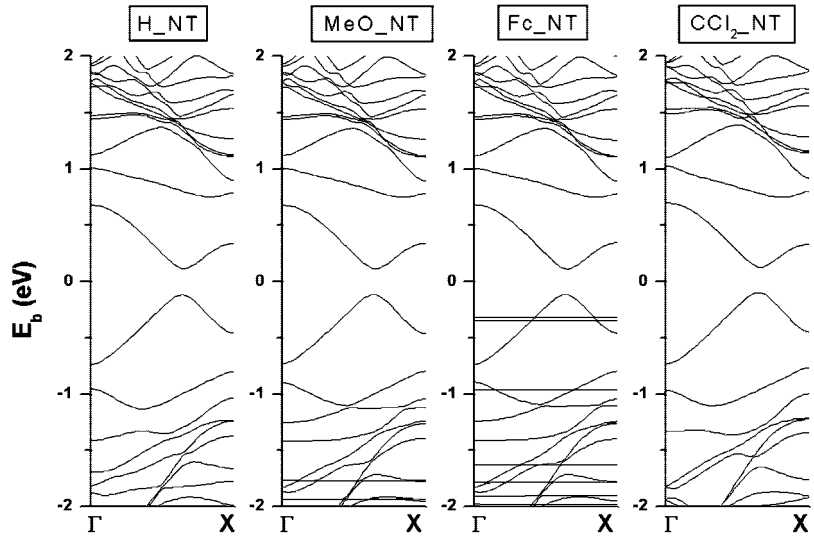

Figure 4. From left to right, the band structures on H_NT, MeO_NT, Fc_NT, and CCl_2_NT are shown. The band structures are calculated for four-unit supercells.

is of interest that the degree of band opening is about 0.23 eV in all functionalized tubes in spite of the difference in functional groups. It reveals that both atomic types of addends covalently attached to the binding segment and the degree of symmetry breaking at the segment, rather than various atoms in the long chain, have crucial influence on the band structures around the Fermi level. For type-B, all functionalized tubes still keep the mirror symmetry of NTs locally, and electronic band structures are similar to those of pristine tubes.

In Figure 5, we examine whether the long chain of azomethine ylide derivatives can freely rotate in a vacuum. For this study, binding energy and time evolution of the torsion angles have been explored with type-A metallic tubes at the Γ point. In Figure 5a, we plot a binding energy profile as a function of torsion angles ϕ(C3−N−C5−C6) after geometry optimizations with the fixed angles at 30° intervals. The energy difference between the maximum and the minimum is 0.3 eV in the (4, 4) tube and 0.2 eV in the (6, 6) tube. From the result of the (6, 6) tube, it can be predicted that comparable binding energies lead to free rotation in the angle range from 60° to 160° at the ambient condition. However, rotation beyond 180° is prohibited because of the energy barrier. In Figure 5b, quantum dynamics simulation has been carried out at 298 K for 8 ps of production run after 2 ps of equilibration in (6, 6) type-A tube with the most stable geometry ($\Phi = 80°$) obtained by Figure 5a as an initial structure. The evolution shows that the torsion angles fluctuate mainly within the range from 60° to 160°, which agrees very well with the result in Figure 5a. After 2 ps of equilibration run, the torsion angle increases up to 180°, then begins to be reduced at about 3.5 ps, and finally oscillates between the angles 40° and 100°. The abrupt change of the angle occurs right after flipping of the pyrrolidine ring at about 3.5 ps. The left snapshot in Figure 5b shows that the nitrogen atom of the ring is on the right side of the plane including two covalent bonds that connect the functional group and the nanotube. The nitrogen atom moves to the left side of the plane after 4 ps as shown on the right snapshot. This ring flip keeps the torsion angle smaller than about 180°.

In Figure 6, we present the band structures of semiconducting (8, 0) MeO_NTs. Unlike metallic tubes, both types show band structures similar to that of the pristine tube around the Fermi level. The changes of band gaps are small (about 0.1 eV) in

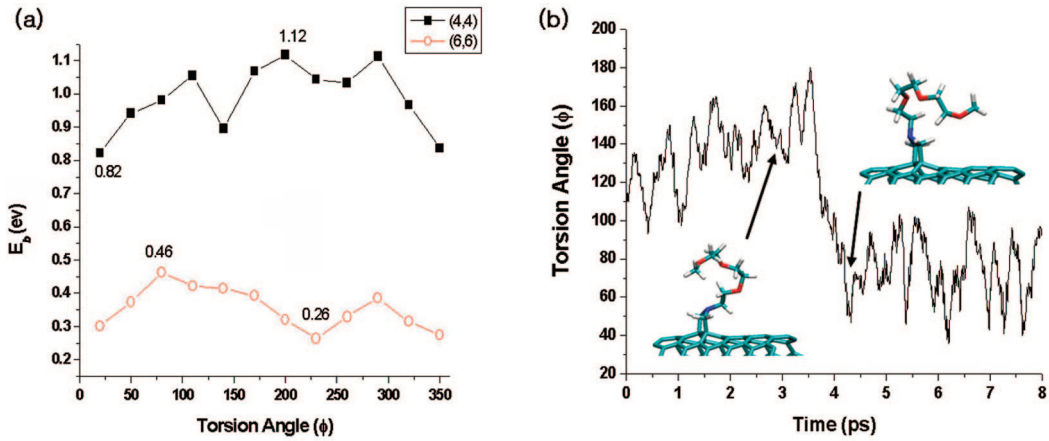

Figure 5. (a) Binding energy profile as a function of the torsion angles after geometry optimizations with the fixed torsion angles at 30° intervals for (4, 4) (solid squares) and (6, 6) (open circles) tubes. (b) Time evolution of the torsion angles for the (6, 6) tube. Snapshots at 2.8 and 4.2 ps represent the configurations of pyrrolidine ring before and after ring flip. CPMD simulations are performed for a six-unit supercell.

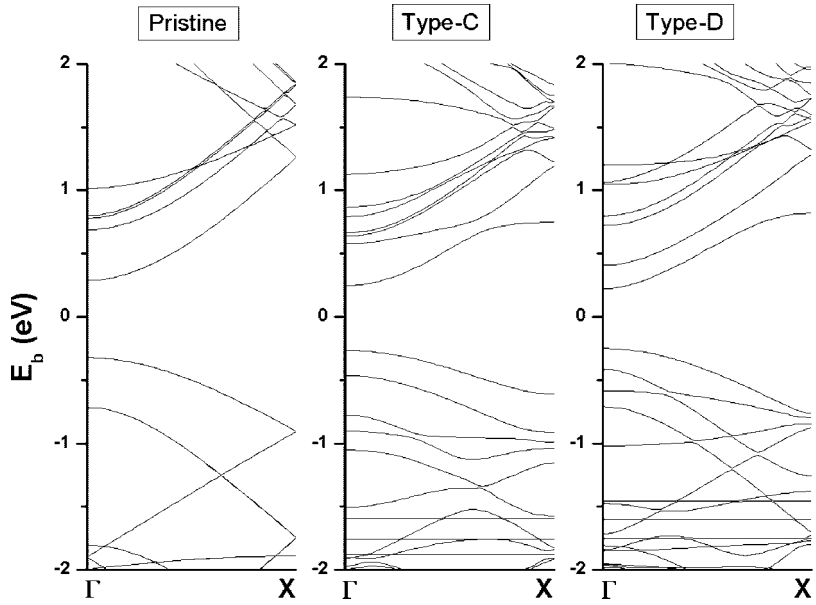

Figure 6. Band structures of pristine (8, 0) nanotube (left), type-C (middle), and type-D (right) zigzag (8,0) MeO_NTs.

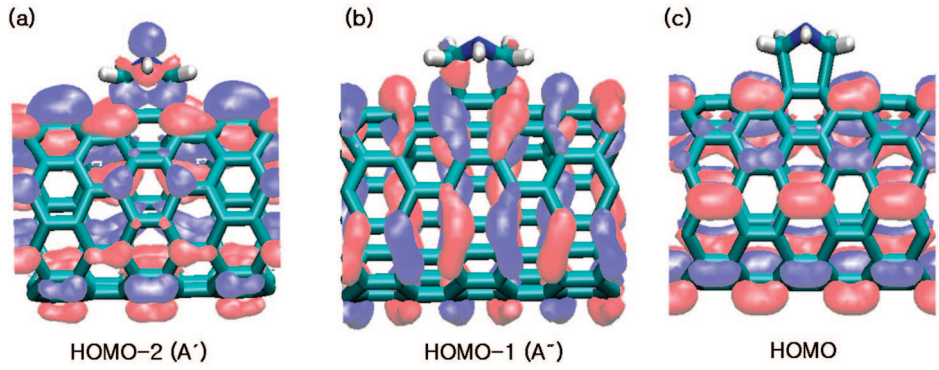

Figure 7. Molecular orbitals corresponding to the (a) HOMO-2, (b) HOMO-1, and (c) HOMO in the semiconducting (8, 0) H_NT.

both types after functionalization, and there are flat bands originating from long organic chains at the position of about 1.5 eV below Fermi energy. Molecular orbitals of the stable type-D configuration in (8, 0) H_NT system are calculated at the Γ points as shown in Figure 7. The molecular geometries of the H_NT system inside the supercell can be described as C_s group.[25] Using this terminology, the highest occupied molecular orbital-1 (HOMO-1) and HOMO-2 can be represented as A'' and A', respectively. Although HOMO-1 and HOMO-2 have different molecular symmetries, both orbitals lead to strong covalent binding between the addend and the NT. On the other hand, neither HOMO nor LUMO (lowest unoccupied molecular orbital) contributes to binding between the addend and the NT, which clearly indicates that the functionalization has little influence on the change of the HOMO−LUMO gap in the semiconducting tubes.

Concluding Remarks

We have investigated the covalently functionalized carbon nanotubes containing azomethine ylides from first-principles. The main purpose is to provide structural and electronic properties of the tubes on the theoretical framework. The results on the binding energies suggest that armchair tubes favor the functionalizaton at the C−C bond slanted to the tube axis (type-A) forming twisted pyrrolidine rings, whereas zigzag NTs prefer the addend attached to the segment parallel to the tube axis (type-D) and generate envelope ring structures. It is also suggested that the geometries of the pyrrolidine ring attached to NTs strongly depend on the binding segment and degree of π-orbital alignment. It is noted that kinetic effects should also be considered for controlling the regioselectivity of 1,3-dipolar cycloaddition of azomethine ylide on NT. It is rather difficult to map out the reaction path and calculate the precise activation energy of the reaction based on the present approach. It was shown that the cycloaddition reaction of azomethine ylide on metallic NT is exothermic (~40 kcal/mol) with a relatively small activation barrier (~3.4 kcal/mol).[19] It can be argued that the barrier heights for the different types of configurations are similar, assuming that the addition reaction proceeds with the same concerted mechanism. Under these conditions, the differences in the binding energies will determine the regioselectivity. One may not rule out the possibility that the cycloaddition follows different pathways depending on the configurations. Further calculations, where different scenarios are examined systematically, will be needed to resolve these issues.

The comparison of various functionalized addends on armchair tubes reveals that the binding segment and atomic types attached to the segment rather than organic long chains have crucial influence on the band structures around the Fermi energy. In metallic tubes, the covalent binding with carbon atoms of the slanted segments of the tubes brings up the band gap opening, whereas the effect of the addends on the change of band gap energy is negligible at any binding segments in the semiconducting NTs. The information obtained from this study may be a stepping stone to steer toward selectively modified carbon nanotubes in nanoscales.

Acknowledgment. E.S. thanks Hee Chol Choi and Cheol Ho Choi for helpful discussions and providing their simulation results prior to publication. This work was supported by the SRC/ERC program of MOST/KOSEF(grant number R11-2005-048-00000-0). S.S. acknowledges support by the Creative Research Initiatives of MOST/KOSEF under contract no. R16-2007-007-01001-0 (2007).

References and Notes

(1) Burghard, M. *Surf. Sci. Rep.* **2005**, *58*, 1.
(2) Pekker, S.; Salvetat, J. P.; Jakab, E.; Bonard, J. M.; Forro, L. *J. Phys. Chem. B* **2001**, *105*, 7938.
(3) Mickelson, E. T.; Huffman, C. B.; Rinzler, A. G.; Smalley, R. E.; Hauge, R. H.; Margrave, J. L. *Chem. Phys. Lett.* **1998**, *296*, 188.
(4) Pan, H.; Feng, Y. P.; Lin, J. Y. *Phys. Rev. B* **2004**, *70*, 245425.
(5) Zhao, J. J.; Park, H. K.; Han, J.; Lu, J. P. *J. Phys. Chem. B* **2004**, *108*, 4227.
(6) Lu, X.; Zhang, L. L.; Xu, X.; Wang, N. Q.; Zhang, Q. N. *J. Phys. Chem. B* **2002**, *106*, 2136.
(7) Holzinger, M.; Vostrowsky, O.; Hirsch, A.; Hennrich, F.; Kappes, M.; Weiss, R.; Jellen, F. *Angew. Chem., Int. Ed.* **2001**, *40*, 4002.
(8) Zhao, J. J.; Chen, Z. F.; Zhou, Z.; Park, H.; Schleyer, P. V.; Lu, J. P. *ChemPhysChem* **2005**, *6*, 598.
(9) Cho, E.; Kim, H.; Kim, C.; Han, S. *Chem. Phys. Lett.* **2006**, *419*, 134.
(10) Ying, Y. M.; Saini, R. K.; Liang, F.; Sadana, A. K.; Billups, W. E. *Org. Lett.* **2003**, *5*, 1471.
(11) Banerjee, S.; Hemraj-Benny, T.; Wong, S. S. *Adv. Mater.* **2005**, *17*, 17.
(12) Xu, Y.-J.; Li, J.-Q. *Chem. Phys. Lett.* **2005**, *412*, 439.
(13) Basiuk, V. A. *J. Phys. Chem. B* **2003**, *107*, 8890.
(14) Georgakilas, V.; Kordatos, K.; Prato, M.; Guldi, D. M.; Holzinger, M.; Hirsch, A. *J. Am. Chem. Soc.* **2002**, *124*, 760.
(15) Guldi, D. M.; Marcaccio, M.; Paolucci, D.; Paolucci, F.; Tagmatarchis, N.; Tasis, D.; Vazquez, E.; Prato, M. *Angew. Chem., Int. Ed.* **2003**, *42*, 4206.
(16) Tasis, D.; Tagmatarchis, N.; Bianco, A.; Prato, M. *Chem. Rev.* **2006**, *106*, 1105.
(17) Bianco, A.; Prato, M. *Adv. Mater.* **2003**, *15*, 1765.
(18) Menard-Moyon, C.; Izard, N.; Doris, E.; Mioskowski, C. *J. Am. Chem. Soc.* **2006**, *128*, 6552.
(19) Lu, X.; Tian, F.; Xu, X.; Wang, N. Q.; Zhang, Q. *J. Am. Chem. Soc.* **2003**, *125*, 10459.
(20) Soler, J. M.; Artacho, E.; Gale, J. D.; Garcia, A.; Junquera, J.; Ordejon, P.; Sanchez-Portal, D. *J. Phys.: Condens. Matter* **2002**, *14*, 2745.
(21) Hutter, J.; Ballone, P.; Bernasconi, M.; Focher, P.; Fois, E.; Goedecker, S.; Marx, D.; Parrinello, M.; Tuckerman, M. E. *CPMD version 3.9.2*; Max Planck Institut fuer Festkoerperforschung Stuttgart, and IBM Zurich Research Laboratory; 1990−2006.
(22) Perdew, J. P.; Burke, K.; Ernzerhof, E. *Phys. Rev. Lett.* **1996**, *77*, 3865.
(23) Dobado, J. A.; Molina, J. M.; Espinosa, R. A. *THEOCHEM* **1994**, *303*, 205.
(24) Niyogi, S.; Hamon, M. A.; Hu, H.; Zhao, B.; Bhowmik, P.; Sen, R.; Itkis, M. E.; Haddon, R. C. *Acc. Chem. Res.* **2002**, *35*, 1105.
(25) Bernath P. E. *Spectra of Atoms and Molecules*; Oxford University Press: Oxford, 1995.

JP710938V